

Characterization of an Independent Fiber Bragg Grating Temperature and Strain sensor in a Germanium-doped Fiber

Marc Phua Hsiao Meng
Catholic Junior College

Dr Michelle Shao Xuguang
Mrs Tay Sue Lynn

The characteristics of an FBG (Fiber Bragg Grating) in response to strain and temperature were recorded. In order to ensure completely different responses to strain and temperature and make it suitable for WDM (Wave-Division Multiplexing) and TDM (Time-Division Multiplexing), 2 separate experiments were conducted. In the first experiment, the Germanium-doped fiber containing the FBG was put in an oven. The FBG was heated in a controlled manner by the oven from temperatures 25°C to 90°C at 5°C intervals. In the second experiment, the FBG was connected to a strain gauge, using a micrometer screw gauge to vary the strain on the FBG. The strain was varied from 0.00 to 0.0196 at constant intervals using 0.0254 cm change in the micrometer screw gauge. The sensitivity of the FBG towards temperature was more than 10 times higher as compared to the strain. The characteristics of Bragg resonance and mode coupling in the fiber sensor were analysed using coupled-mode theory.

I. INTRODUCTION

The FBG in the current scientific field is one of the most commonly used sensors in the world due to its many advantages such as its simplicity for wavelength encoding [1], and ability to control the grating pitch, amplitude, Bragg resonance and chirp of the Bragg grating. It is highly regarded and considered to be one of the essentials that can be further exploited for use in optical devices such as WDM (Wave-division Multiplexing) and TDM (Time-division Multiplexing) optical communication and sensing devices [3,4]; optical fiber sensors for measuring temperature and strain changes in any walk of life such as building damage, medical [5], civil engineering, radiation leaks [2], high pressure detection [2], oil and gas applications [2]. FBG temperature and strain sensors offer high sensitivity, real-time stability [1], has immunity to electro-magnetic interference [1,3] and has ability for multiplexing [1]. Furthermore, Germanium, doped inside the fiber's core is commonly known to raise the refractive index of the silica-clad core due to its higher photosensitivity, which means that the refractive index of the core changes with exposure to UV light. The amount of the change depends on the intensity and duration of the exposure as well as the

photosensitivity of the fiber. This causes the fiber to be more sensitive to temperature and strain shifts with doping increasing the sensitivity of the fiber up to 10 times its original value due to the increased reflectivity of the FBG.

When light of high intensities is shone along the fiber core, there is an increase in the refractive index, giving rise to Bragg resonance. Due to the low coefficient of linear thermal expansion of both silica and Germanium, there is no temperature-induced strain on the FBG. Hence, it could function as an independent sensor for either temperature or strain assessments.

Technically, these fiber sensors are able to sense either a shift in temperature or strain with great accuracy. However, sometimes there may be discrepancies between each effect. This is commonly known as temperature-strain discrimination [5], whereby the effects of both strain and temperature cause Bragg resonance at the same instance. It could be impossible to determine the exact cause of the strain if the FBG had both similar responses to both strain and temperature.

However, if the FBG differed greatly in their responses to each effect, the Bragg

wavelength shifts due to each effect could be found using a matrix representation from data collected by collocated sensors at the same point on the structure [5]. This can be useful for temperature fluctuation during the day, so as to enhance its multiplexing capabilities and system performance accuracy.

The aim of this experiment was to test if a FBG in an Germanium-doped single mode fiber was able to function as an independent temperature or strain sensor for WDM and TDM capability for practical use such as heat sensing, human movement sensing and traffic sensing in harsh environments.

The fiber I used was placed under standard conditions with various fluctuations in temperature and strain. The significant difference in Bragg resonance in correspondence to shifts in strain and temperature by the FBG was remarkable.

II. THEORY

Coupled-mode theory is a theory for obtaining quantitative information about the diffraction efficiency and spectral dependence of fiber gratings. In the ideal-mode approximation to coupled-mode theory, we assume that the transverse component of the electric field can be written as a superposition of the ideal modes labeled (i.e., the modes in an ideal waveguide with no grating perturbation), such that:

$$\vec{E}_t(x, y, z, t) = \sum_j [A_j(z)e^{iB_j z} + B_j(z)e^{-iB_j z}] \cdot \vec{e}_{jt}^*(x, y)e^{-i\omega t} \quad (1)$$

where $A_j(z)$ and $B_j(z)$ are slowly varying amplitudes of the j^{th} mode traveling in the Z^+ and Z^- directions, respectively.[6]

The transverse mode fields $\vec{e}_{jt}^*(x, y)$ might describe the bound-core or radiation LP modes, as given in (1), or they might describe cladding modes. While the modes are orthogonal in an ideal waveguide and hence, do not exchange energy, the presence of a dielectric perturbation causes the modes to be coupled such that the amplitudes and of the j^{th} mode evolve along z the axis according to

$$\frac{dA_j}{dz} = i \sum_k A_k (K_{kj}^t + K_{kj}^z) e^{i(B_k - B_j)z} + i \sum_k B_k (K_{kj}^t - K_{kj}^z) e^{-i(B_k + B_j)z} \quad (2)$$

$$\frac{dB_j}{dz} = -i \sum_k A_k (K_{kj}^t - K_{kj}^z) e^{i(B_k + B_j)z} - i \sum_k B_k (K_{kj}^t + K_{kj}^z) e^{-i(B_k - B_j)z} \quad (3)$$

In (2) and (3), is the transverse coupling coefficient between modes and given by

$$K_{kj}^t(z) = \frac{w}{4} \iint dx dy \Delta \varepsilon(x, y, z) \vec{e}_{kt}(x, y) \cdot \vec{e}_{jt}^*(x, y) \quad (4)$$

where $\Delta \varepsilon$ is the perturbation to the permittivity, approximately $\Delta \varepsilon = 2n\delta n$ when $\delta n \ll n$. The longitudinal coefficient, $K_{kj}^z(z)$ is analogous to $K_{kj}^t(z)$, but generally $K_{kj}^z(z) \ll K_{kj}^t(z)$ for fiber modes, and thus this coefficient is usually neglected. [6]

In most fiber gratings the induced index change $\delta n(x, y, z)$ is approximately uniform across the core and nonexistent outside the core. We can thus describe the perturbed core index $\delta n_{co}(z)$ due to a varying pattern of UV light, to be described as:

$$\delta n_{co}(z) = \overline{\delta n_{co}}(z) \left\{ 1 + v \cos \left[\frac{2\pi}{\Lambda} z + \phi(z) \right] \right\} \quad (4)$$

where $\overline{\delta n_{co}}(z)$ is the “dc” index change spatially averaged over a grating period, v is the fringe visibility of the index change, Λ is the normal period, and $\phi(z)$ describes grating chirp.[6] If we define two new coefficients

$$\sigma_{kj}(z) = \frac{wn_{co}}{2} \overline{\delta n_{co}}(z) \iint dx dy \vec{e}_{kt}(x, y) \cdot \vec{e}_{jt}^*(x, y) \quad (5)$$

$$k_{kj}(z) = \frac{v}{2} \sigma_{kj}(z) \quad (6)$$

where σ is a “dc”(period-averaged) coupling coefficient and k is an “AC” coupling coefficient, then the general coupling coefficient can be written

$$K_{kj}^t(z) = \sigma_{kj}(z) + 2k_{kj}(z) \cos \left[\frac{2\pi}{\Lambda} z + \phi(z) \right] \quad (7) \quad [6]$$

III. EXPERIMENT

A Bragg grating is a periodic structure fabricated through a series of mechanical translations through exposing the core of the fiber to ultraviolet light using a phase mask. When light from the optical broadband source interacts with a grating, a single wavelength, known as the Bragg wavelength is then reflected down the fiber. The equation to describe this phenomenon would be;

$$\lambda_B = 2n_{eff}\Lambda \quad (8)$$

where Λ is the grating pitch and n_{eff} is the effective refractive index of the fiber. Both of these factors depend on the temperature and strain applied to the fiber core. The effective refractive index of the fiber can also be defined as:

$$n_{eff} = n(1 + \Delta b) \quad (9)$$

with Δ being the fractional core-cladding refractive index variation while b is the normalized modal parameter [7]. This is also known as the refractive index of the mode propagating in the fiber. When strain or temperature produces an expansion of the fiber core, the Bragg wavelength is shifted, as there would be a change in the effective refractive index. The shift due to both these effects can be written as:

$$\Delta\lambda_B = 2n_{eff}\Lambda \left\{ \left(1 - \frac{n^2}{2}\right) [P_{12} - \nu(P_{11} + P_{12})] \right\} \Delta\varepsilon + \left[\alpha + \frac{dn}{dT} \right] \Delta T \quad (10)$$

where ε is the applied strain, P_{11} and P_{12} are the Pockel's coefficients of the stress optic tensor, ν is

Poisson's ratio, and α is the coefficient of thermal expansion of the fiber material, in this case, silica, and ΔT is the temperature change [4]

The approach to remove temperature-strain discrimination is to locate two sensor elements which have very different responses to strain ($K\varepsilon_1, K\varepsilon_2$) and temperature (KT_1, KT_2) at the same point on the structure (collocated sensors). Then a matrix equation:

$$\begin{pmatrix} \Delta\lambda_1 \\ \Delta\lambda_2 \end{pmatrix} = \begin{pmatrix} K\varepsilon_1 & KT_1 \\ K\varepsilon_2 & KT_2 \end{pmatrix} \begin{pmatrix} \varepsilon \\ T \end{pmatrix} \quad (11)$$

can be written and inverted to yield strain and temperature from measurements of the two wavelength shifts whereby $\Delta\lambda_1$ is the Bragg wavelength shift due to change in

strain while $\Delta\lambda_2$ is the Bragg wavelength shift due to change in temperature. The success of this technique depends on the ratio of the strain responses of the two sensors being different from the ratio of their temperature responses, so that the determinant of the matrix $\begin{pmatrix} K\varepsilon_1 & KT_1 \\ K\varepsilon_2 & KT_2 \end{pmatrix}$ is non-zero: [4]

$$\frac{1}{K\varepsilon_1KT_2 - K\varepsilon_2KT_1} > 0 \quad (12)$$

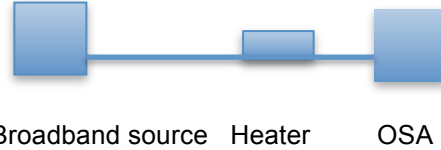


Figure 1. Experimental setup for temperature sensitivity measurement

Figure 1 shows the experiment setup used to measure temperature sensitivity of the proposed FBG sensor. A single-mode fiber containing an FBG of grating pitch 1064.76nm was heated using a heater (HCP MOV003023011) and connected between an optical broadband source (Infinon Research SLED broadband light source (IRBL-11111-F)) and an optical spectrum analyzer (YOKOGAWA AQ6370C). Temperature was varied from 25 °C to 90 °C at 5°C intervals in a controlled manner using the heater without any strain applied.

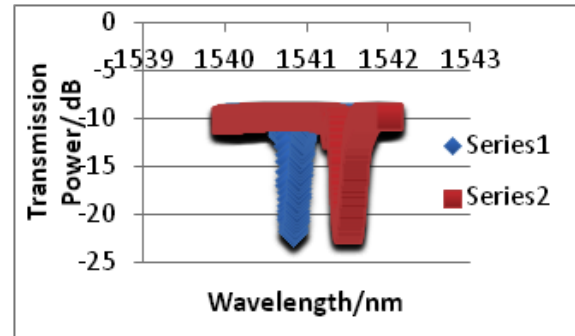


Figure 2. Spectral response of the proposed FBG sensor due to corresponding temperature
Figure 2 shows the spectral response of the fabricated FBG temperature sensor when placed in an oven at 25°C and 90°C. Series 1 shows the spectrum at 25°C while series 2 shows it at 90°C. The Bragg wavelengths were 1540.8nm at 25 °C and 1541.5nm at 90 °C respectively.

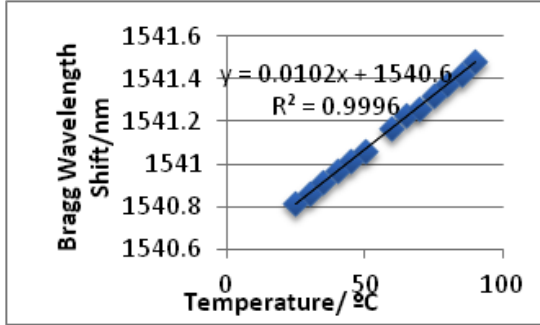
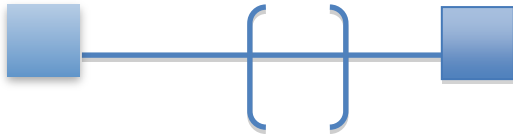


Figure 3. Temperature sensitivity of the proposed FBG sensor

Figure 3 shows the temperature of the fabricated FBG sensor placed in an oven against the Bragg wavelength of the FBG to measure the temperature sensitivity of the FBG sensor. The Bragg wavelength shift was 0.7nm from 25 °C to 90 °C, corresponding to a temperature sensitivity of 0.0102nm/°C. Furthermore, the sensitivity of the temperature-independent FBG sensor can be represented as:

$$\frac{1}{\lambda_B} \frac{\partial \lambda_B}{\partial T} = 6.58 \times 10^{-6} \text{ } ^\circ\text{C}^{-1}$$

whereby a wavelength resolution of ~1pm(0.001nm) is required (at $\lambda_B=1.3\text{nm}$) to resolve a temperature change of ~0.1°C [4].



Broadband Source Strain Gauge OSA

Figure 4. Experimental setup for strain sensitivity measurement

Figure 4 shows the experimental setup used to measure strain sensitivity of the proposed FBG sensor. A strain gauge was applied to an identical fiber as the one stated above, using a micrometer screw gauge to vary the strain on the FBG (strain gauge). The strain gauge is connected between the same optical broadband source and the same optical spectrum analyser. The strain was varied from 0.00ε to 0.0196ε at constant intervals of a 0.0254 cm change in the micrometer screw gauge.

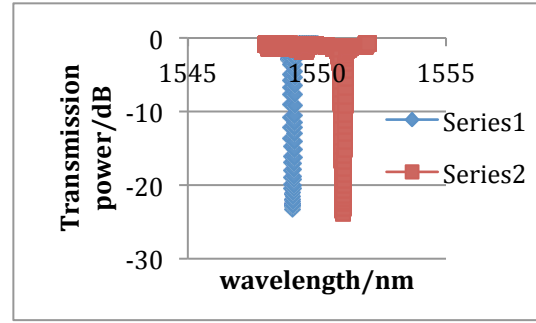


Figure 5. Spectral response of the proposed FBG sensor due to corresponding strain

Figure 5 shows the spectral response of the fabricated FBG strain sensor when placed in a strain gauge, with strain varied from 0.00ε to 0.0196ε. Series 1 shows the spectrum at 0.00ε while series 2 shows the spectrum at 0.0196ε. The Bragg wavelengths were 1549.08nm at 0.00ε and 1551.0nm at 0.0196ε respectively.

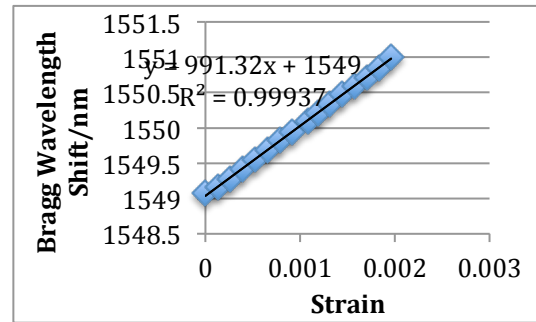


Figure 6. Strain sensitivity of the proposed FBG sensor

Figure 6 shows the strain applied on the FBG strain sensor by the strain gauge against the Bragg wavelength shift of the FBG to measure the strain sensitivity of the FBG sensor. The Bragg wavelength shift was 1.92nm from 0.00ε to 0.0196ε, corresponding to a strain sensitivity of 991.32nm/ε, so at 1549.08nm, the strain sensitivity was (±0.1)1.00pm/με. This can also be expressed as:

$$\frac{1}{\lambda_B} \frac{\partial \lambda_B}{\partial \epsilon} = 0.64 \times 10^{-6} \text{ } \mu\epsilon^{-1}$$

whereby the grating shift with strain measurement is (±0.01) 1nm per ~1000 με at a Bragg wavelength of ~1.3nm.

IV. CONCLUSION

To test if the FBG could function as an independent temperature or strain sensor,

we put one FBG sensor in an oven (heater) and heated it to various temperatures to test for temperature sensitivity while we connected another separate FBG sensor to a strain gauge and varied the strain applied on the FBG to get strain sensitivity. The temperature sensitivity was $0.0102\text{nm}/^{\circ}\text{C}$ which was more than 10 times higher than the strain sensitivity which was $1.00\text{pm}/\mu\epsilon$. Thus, this ensures an FBG sensor fabricated in a Germanium-doped fiber has a very different ratio of strain responses to temperature responses and is able to function as an independent temperature or strain sensor and is suitable for WDM and TDM due to the removal of temperature-strain discrimination, making it more adaptable for accurate detection of temperature or strain change in a harsh environment where these 2 systems usually are placed in. Possible future studies in fields related to this area would be body measurement, goal-line technology and bank security detection systems as all of them require strain sensing to accurately detect the presence of an object or a person or to fit the exact body specifications while only bank security detection systems require temperature sensing to detect smoke or fire near the bank vault and strain sensing to detect access to restricted areas.

Furthermore, a body measurement system can be improved further by mapping this technology into a suit, for exercising, allowing users to also detect their body temperature, running velocity and acceleration through temperature and strain shifts of the FBG respectively. This suit could essentially be a multipurpose suit, designed for various specifications such as combat training, underwater naval diving with its limitless possibilities. Firstly, the suit has the ability to measure heart rate with its high strain sensitivity being able to detect changes in the heart pulse. Secondly, divers can use this suit to detect pressure increase when diving, ensuring when to keep they're level or descent further.

Lastly, the FBG could be an essential temperature sensor when trying to incorporate a new thermoelectric effect into commercial cars. This effect involves the use of the cars excess engine heat to be converted into electrical energy. This

process is also known as the Seebeck effect whereby a gradient in temperature between a warmer and colder side generates electricity. The FBG can be implemented to detect excess temperature in the interior parts of the car using WDM to encompass the entire car and when a Bragg wavelength shift is detected due to excess temperature, a switch used to control the entire electricity-generating circuit will close, causing the Seebeck effect to take place whereby an internal Electric field generated from the hot end to the cold end will be able to flow an entire circuit essentially powering the car.

ACKNOWLEDGEMENTS

This work was supported by the Nanyang Research Programme 2014 and supervised by Dr Michelle Shao Xuguang and Dr Wu Zhifang.

REFERENCES

- [1] Cheri-Hee Lee, Jonghun Lee, Min-Kuk Kim and Kwang Taek Kim, 2011. Characteristics of a Fiber Bragg Grating Temperature Sensor Using the Thermal Strain of an External Tube. Journal of the Korean Physical Society, Vol. 59, No. 5, pp. 3188~3191
- [2] Stephen J. Mihailov. 2012. "Fiber Grating sensors for Harsh Environments", Sensors 2012, 12, 1898-1918; doi:10.3390/s120201898
- [3] Dr Crispin Doyle, 2003. "Fibre Bragg Grating Sensors, An Introduction to Bragg gratings and interrogation techniques"
- [4] Alan D. Kersey, Michael A. Davis, Heather J. Patrick, Michel LeBlanc, K. P. Koo, Member, IEEE, C. G. Askins, M. A. Putnam, and E. Joseph Friebele, 1997. "Fiber Grating Sensors", Journal Of Lightwave Technology, Vol. 15, No. 8, August 1997
- [5] Y. J. Rao, D. J. Webb, D. A. Jackson, L. Zhang, and I. Bennion, 1998. "Optical In-Fiber Bragg Grating Sensor Systems for medical applications", Journal Of Biomedical Optics 3(1), 38-44 (January 1998)
- [6] Turan Erdogan. "Fiber Grating Spectra", Journal Of Lightwave Technology, Vol. 15, No. 8, August 1997
- [7] Richard J. Black, David Zare, Ilevy Oblea, Yong-Lae Park, Behzad Moslehi, and Craig Nelsen. "The Gage Factor For Optical Fiber Grating Strain Gages", Intelligent Fiber Optic Systems Corporation (IFOS)

